

# Detecting Sugarcane Crop Yield using Decision Tree Classifier in the District of Muzaffarnagar

Ankit Kumar<sup>1</sup> and Anil Kumar Kapil<sup>2</sup>

<sup>1</sup>Research Scholar, Faculty of Mathematics and Computer Sciences, Motherhood University, Roorkee, INDIA

<sup>2</sup>Professor, Faculty of Mathematics and Computer Sciences, Motherhood University, Roorkee, INDIA

<sup>1</sup>Corresponding Author: [ankitsiet103@gmail.com](mailto:ankitsiet103@gmail.com)

## ABSTRACT

The district of Muzaffarnagar is the highest sugarcane producing district in Uttar Pradesh and therefore is an important industrial district as well. The district is part of Western UP and it shares the problems of the sugar industry elsewhere in the state: unpredictable demands and crop failures. In this context, predicting sugarcane demand and informing its production can turn to be just the key to solve some of the problems the industry faces.

The existing crop forecasting method for the cultivation of sugarcane used in UP relies, to a large degree, on subjective details, centred on the expertise of engineers in the sugar and alcohol field and on information on input demand in the supply chain. The measurement of the utility of the sample detection using NDVI images from the SPOT sensor used in the sensor's determination over the ECMWF model was possible to infer the official productivity data reported in the previously selected municipalities and harvest. Significant features of the municipal productivity of a given village is listed in a decision tree, and out of the combinations of attributes the corresponding municipal productivity is rated as "Normal" on the average urban productivity scale. Using data from the NDVI time-series between 2013 to 2020, we can discern the three classes of productivity in the meanwhile. Findings indicate that productivity in January ranked as less than mean, mean, and more than mean. The findings were more successful for the class Vegetation, the participants of which were permitted to conclude about the pattern of the average federal productivity prior to.

**Keywords**— Crop, Decision Tree, Sugarcane, Muzaffarnagar

credit and sugar mills in the state owe in lakhs of crores to farmers. This is because the industry is highly vulnerable to fluctuations in demands in the domestic and international markets as well as because the crop itself is susceptible to failure due to insect and unfavourable climate.

It is situated midway on Delhi-Haridwar/Dehradun National Highway and falls under the Western Uttar Pradesh region. The district is situated in the centre of extremely productive upper Ganga Yamuna Doab area and is very close to the New Delhi as well as Saharanpur, indicating that it is one of the most modern and wealthy citizens in Uttar Pradesh. It is under the Saharanpur division of police. The city also has a rather strong geographical significance, as it shares its frontier with the state of Uttarakhand and is the principal economic, financial, industrial and educational hub of Western UP.

On the seasonality section, it is summer season, and as it is in Muzaffarnagar, it has the humid subtropical climate with warmer summers and colder winters. Summers last from early April to late June, are very sunny, and are very stormy. By early June, the monsoon has arrived in the area and goes on into late September. It dawns slightly, with a decent amount of cloud cover but with higher humidity amounts. The spring is normally warm and dry during the months of September and October but cold and damp from the middle of October to the middle of March. The month of June is the warmest month of the year with a temperature of 30.2 degree Celsius. January, the annual average temperature for 2014 is 12.5 degrees Celsius. The temperature for this year is the lowest for the entire year. The average annual temperature in the village of Muzaffarnagar is 24.2 degrees Celsius. The total annual rainfall here is 968 mm. The maximum precipitation happens in July, with an average of 261.4 mm of rain.

Muzaffarnagar is the largest sugarcane producing district in UP. The existing crop forecasting method for the cultivation of sugarcane used in UP relies, to a large degree, on subjective details, centred on the expertise of engineers in the sugar and alcohol field and on information on input demand in the supply chain. The measurement of the utility of the sample detection using NDVI images from the SPOT sensor used in the sensor's determination over the ECMWF model was possible to infer the official productivity data reported in

## I. INTRODUCTION

Uttar Pradesh is the largest sugarcane producing state in India with more than 38 per cent share in the total national production (Government of India, 2019). Sugarcane farming covers over 22 lakh hectares of land in the state and employs lakhs of labours and sugarcane farmers. Over a period of time, while the sugar industry of other states such as Maharashtra and Telangana employed modern machineries, those in the Uttar Pradesh couldn't. As a result of this, the sugar recovery rate and production per hectare of land in Uttar Pradesh are lower than those of some of the advanced states such as Maharashtra and Telangana. The industry also runs on

the previously selected municipalities and harvest. Significant features of the municipal productivity of a given village is listed in a decision tree, and out of the combinations of attributes the corresponding municipal productivity is rated as "Normal" on the average urban productivity scale. Using data received by the NDVI time-series between 2013 to 2020, we can discern the three classes of productivity in the meanwhile. Findings indicate that productivity in January ranked as less than mean, mean, and more than mean. The findings were more successful for the class Vegetation, the participants of which were permitted to conclude about the pattern of the average federal productivity prior to.

## II. BACKGROUND & LITERATURE REVIEW

Sugarcane is a spreading limbed tropical woody plant of 2 to 6 metres high that is grown in areas all over the tropical and subtropical worlds. The sugarcane develops in two steps, first, as a fruit, then as a ratoon.

- **Germination phase:** The sugarcane begins to germinate about three weeks post seeding.
- **Tillering phase:** Whereas, in time, such process begins up after two months, and the tillers to come out of the base of roots are five to ten stalks that remain steadfast.
- **Grand growth phase:** The first two stages last 120 days and it is the third period of time that decides when the star fruit is ready. Stabilization of the tillers depends on the onset of the seedlings early on in their development. But one of the tractors produced did not make it to harvest time, and also the farmer harvested less than half the amount of seeds. The yield of the plant hits its highest during the fourth of fifth phase of its growth. Development of the stalk is seen to be very rapid at this point, resulting in the formation of 4 to 5 internodes in a month. Finding the right time for classifying the sugarcane crop by satellite false colour composite imagery is a good time.
- **Maturity or ripening phase:** In this point, deposition of sugar may be unmistakable at the broken network junctions. Often, we can see that the moisture content significantly declines from 85 to 70 percent as maturity occurs.

### *Remote Image Sensing Approach based on Decision Tree Classifier*

In remote sensing methods, such as imaging, the sensors usually do not actually get in touch with the original object, however, this approach does allow for an impartial and unaltered image of the original object without the sensor impacting the original object. Although there is no immediate or physical touch, the input comes from the target to the sensor to the electrode and then up into the electromagnetic field. When it comes to these measures, there are a few metres apart

(beam length) from instruments and a few miles apart (distance it travelled) from a jet. These measurements are often taken from a few thousand to a few million miles away by satellite (Lillesand & Kiefer, 1987; Joseph, 2003). Time-consuming, expensive and very lethal, aerial and land surveys are unreliable and don't often produce reliable results. Remote sensing methods, however, are fast, simple and convenient. They can be used to get data from a particular location that is inaccessible and hazardous (Gautam & Mehta, 2015). The technique known as "remote sensing" lets mapping of huge plots of land in an easy manner, but without full precision.

Narciso & Schmidt (1999) showed the possibility of combining the ETM+ results and the Ladner et al. (1987) classification methodology for a number of items like sugarcane crops and mulberries in Estonia, southern Africa. According to Markley, et al. (2003), the cultivated cane crop in Australia could be correctly measured using a SPOT and LANDSAT images. There are few points of concern in the quote above. First, it's a fascinating, but lengthy, source. Second, the actual source is provided in the "show citations" direction at the bottom of the paragraph ... This version may be outdated. Third, the "show citations" direction is a smart choice for most quotations. Initially, they downloaded NDVI plots for different crop styles, including sugar cane, and found positive values ranging from 0.23 to 0.56 for each plot.

### *Time Series Analysis of Spot Vegetation Images*

To forecast sugar cane production for a given area, individual sugar mills may perform a basic math amount within their own region. Even though the projections of how much sugarcane sugarcane yields present a subjective factor, they are considered reliable because data collected in the survey are based on information collected from farmers by means of queries, on historical information about how much things cost in previous years, on observations about how much things can differ in the field, and on data about changes in sugarcane production gathered during field work (IBGE, 2002; CONAB, 2007).

The author is of the opinion that it would be better to research this plant on a regional scale, so that farmers across the area know how to harvest the plants for their economic own and to glean knowledge about the plants in any production, before they are harvested. Like a low spatial resolution traditional sensor, a low scalar autonomous information mobile (base station), have been showing to be appropriate for remote monitoring which aims at production evaluation. In this experiment, researchers are gathering and evaluating data from all various areas. The ultimate aim of the study is to establish what the life cycle is like of an unknown plant species from an isolated area. As seen in the plantation yield detectors, these have become sufficient for the purpose of production prediction. To denote the growth and production of agriculture in Brazil, simulation of agricultural yield over time is underway by

the Method of Observation by Fernandes et al. (2004), that helps us to detect in which season a field is more heavily cultivated. are being seen to clearly provide enough figures for seeding at production tracking aimed at yield calculation. They calculate the activities of the vegetation based on the satellite imagery; the Digital Infrared Index (NDVI) time series made from the Method of Observation by Fernandes et al. la Terre (SPOT) Vegetation model. The simulation will generate results that can be compared with the average agricultural yield in a town or parcel of land.

### III. MATERIAL & METHODS

Study focused on local farmers who planted rice crops to investigate the impact of pesticide application

on various soil types. In the IBGE data for sugarcane, the average municipal yield numbers were collected (2008). Owing to the fact that the SPOT Landscape photographs were made available in August 2018, this span is just the months of August and October of 2018 and the two months of August and September of 2019. The SPOT Vegetation provides free low spatial resolution NDVI images (daily), making Sentinel-1 the first satellite to deliver this capability (Vegetation, 2007). The study had access to 255 separate photographs taken from the SABER instrument used by NASA.

The next meteorological variable was rainfall, where the rainfall was split into 11 separate 10-day cycles, the average of which was estimated to form the rainy ten day cycle.

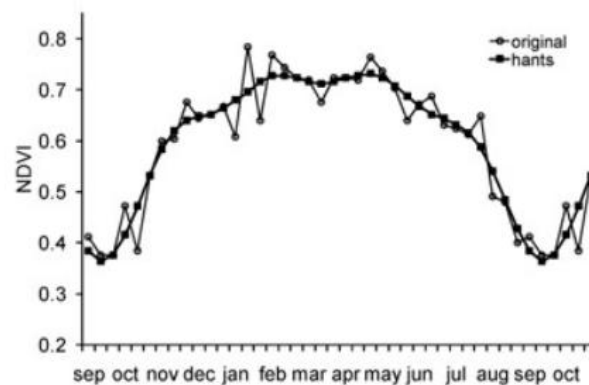


**Figure 1:** Example of Hants' algorithm for a pixel in sugarcane cultivation, applied on 10-day SPOT Vegetation images

Other two meteorological variables were Global radiation and cumulative value for 10-day periods. Other than latitude and longitude, the NDVI and MET data were obtained from the current time frame starting from 2018 and running until 2020. To control for possible cloud impacts. According to the researchers, Roerink et al. (2000) briefly evaluates attributes such as the NDVI temporal activity during the growing season as an up and down in development. Because of that, the sequence was changed by suppressing high frequency noise that was deemed meaningless. The modification was based on a minimal amount of quadric practical error. As an example, take what would happen to a pixel's values if there was a shift in sugarcane cultivation, and modify them (up or down).

This research was conducted using a Geographic Information System (GIS) to look at sugarcane fields that are found only in sugarcane fields in the areas of study. From the CANASAT (2007) teratological map, an area map from maize, tobacco, and sugar cane were drawn and planted coloured sugarcane in the areas coloured it. Section 2 then, the NDVI time series profiles were collected from each chosen pixel in all territories and cropping seasons.

The average monitoring time series profile was built and yielded now projections of the crop yields. By averaging the noise profiles, the spectral data has been

scaled down to be sufficient in the qualitative details required for the input. There is no reported daily weather for each municipality. Instead, they use weekly averages of meteorological readings from the national weather service. A method for image data extraction was rendered by using the ENVI computational system or the IDL computational system based on the analysis carried out by Esquerdo et al. in all of the 4 images (2006). The defined technique of Lucas et al. relates to how plants are classified as successful (Stable state, established) during the vegetative development stage, then on the next leg during the flowering / senesce stage, and finally on the third leg during the formal harvest and extraction (2005a). The accelerated development of the embryo was split into two parts: quick growth and slow growth. Thus, instead of having one key model, the development adopted 4 separate phases: establishment, rapid growth, slow growth, and stability / senesce. With 20 municipalities as the sample collection, the amount of nitrogen is closely tracked from season to season, and a median pattern from 20 seasons was analysed and compared to determine the production of plant richness for each cropping season. The phenological stages of crop production were described in record vegetation growth data, based on observations of a general activity of NDVI data for seven years. After taking all the readings, the NDVI measurements among each cropping

season are shown in the above image. Top row: average, middle row: standard deviation, bottom row: sum of the squares of standard deviation. Then, NDVI and meteorological data were collated by phase, and the spectra of light and the meteorological modelling were

conducted for each development phase, and the attributes of light, wind, and temperature at each development phase, emphasising that summer is the crop development stage with the most spatially uniform attributes.

**Table 1:** Limits of classes for the average municipal yield and number of occurrences

Class	Description	Lower limit t ha <sup>-1</sup>	Upper limit	Frequency
Low-medium	61	72	25	B-M
Medium	75	84	75	M
Medium-high	87	111	41	M-A

The accompanying graph illustrates how the statistics tables demonstrate how these figures were obtained as well as the lower and higher limits of the sample sizes of these statistics and the number of instances. A programme package called Weka was employed to study the features collected and classified. There were four techniques used for function selection: After the above filtering process, Our goal was to discover the kinds of attributes were chosen by the plurality of approaches, which of those attributes were the most important to decide the average regional yield attribute.

To check the trend seen in the 2 ma correlation study, two approaches were taken (a) using spectral attributes and (b) using the average geographic yield. The first method considered the average crop yield for each season, considering the average crop yield in each field. To measure the average spectral attribute (like light, colour or sound) and the average crop yield among the regions, one gathered all the data (the number of crops planted in each location) for each particular area and crop system. In order to analyse the average crop

yields annually, crops were analysed on a yearly basis, not just a three year cycle. The average historical value of spectral attributes and yields was determined with the aid of all the municipalities.

#### IV. RESULT AND DISCUSSION

A table below the "Improvements" column displays the chosen characteristics for each enhancement process. The meteorological characteristics were chosen, but by accident. It is likely that as a result of fixing the development phases on the calendar for 2008, the development phases for 2009, 2010 and 2021, as well as the by implication of accumulated meteorological results, were predetermined. The explanation that the yield is not reported is due to the imprecise procedure for discretization employed within this lab. In doing primary analysis with percentiles system in place, the three groups in percentiles did not catch the numeric choice score well.

**Table 2:** Selected attributes for each attribute selection method

Attributes	Phase	Selection Methods			
		1	2	3	4
ndvi_1final	1		x		
ndvi_1m	2	X		X	X
ndvi_2final	2	X		X	X
ndvi_3s	3	X		X	X
ndvi_3inic	3	X	X	X	X
ndvim	Whole crop	X		x	X
ndvimax			x		
Decmax		x			x

Based on the above properties, the J48 category program was implemented using a decision tree. The cross validation approach was introduced by 5-folds, and it had the consequence of successful prediction. In 140

applications, the classifier accurately predicted 70% of the time, taking the error rate down to 40%. The following table provides a summary of it.

**Table 3:** Confusion matrix and classification accuracy for yield rate from ndvi2\_m, ndvi2\_final, ndvi3\_s, ndvi3\_inic and ndvi\_m attributes

Classification/Original	B-M	M	M-A	Accuracy [%]
B-M	14.5	10	2.2	63%
M	6.4	54	12.5	74%
M-A	3	9	27	67%

It was found that there was a lack of balance between the results, with more uncertainty occurring between neighbouring classes than between distant classes. It is possible that there is a misunderstanding involved with the way that the attribute value class is specified (average crop yield). The primary purpose of the ndvi2 final and ndvi2 m features is to convert the output of the tree level feature extraction stage to a higher level feature-vector (NDVI2 VEC). These groups are the fastest rising sub-sections of the group, gathered

during the growth process means that the area of crops will be able to generate more high quality yields.

Then, a new classification was done by using 160 instances, which did not include the code "89" and which contained 15 instances of the code "62". In order to create a methodology to better distinguish the dataset, the J48 classifier algorithm was used with ten items required, and cross validation was used with five folds for the training collection. If you had to score the classifier on reviewing 66% of the cases, you could infer that 94 out of 140 instances were correctly guessed.

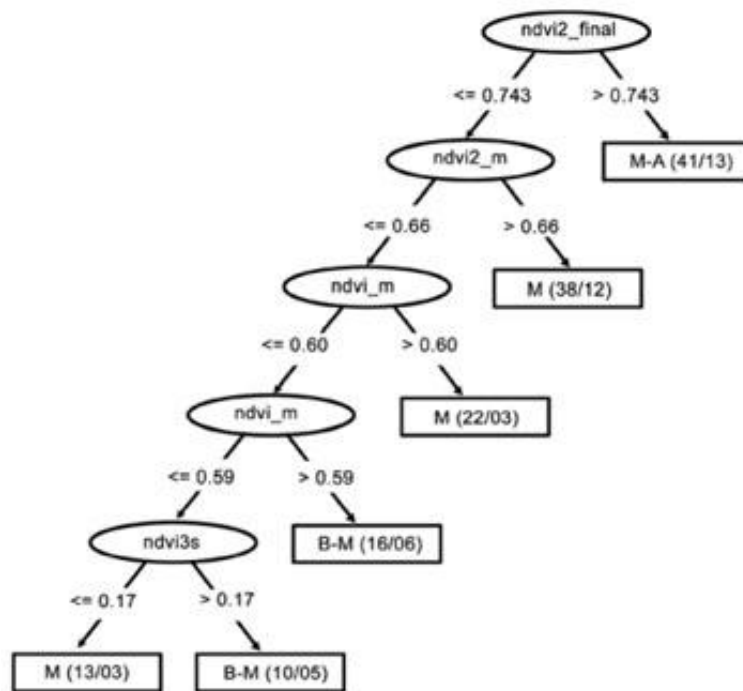


Figure 2: Decision tree for yield classification using ndvi2\_m, ndvi2\_final, ndvi3\_inic and ndvi\_m attributes

Although there was a substantial deterioration about the classification of yield BM, whose hit percent decreased from 62.5 to 8.3. The study's results classified M class yield increased from 74.3% to 86.5%. It's

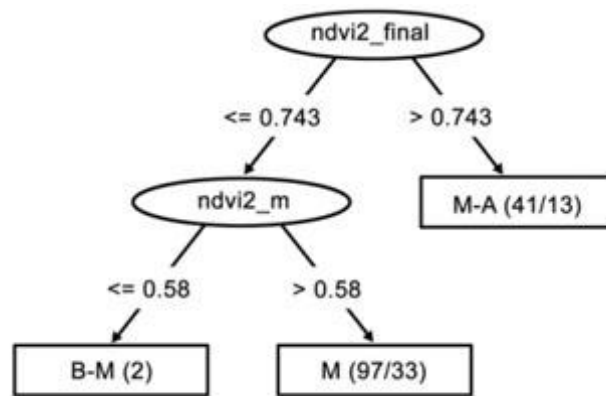
accuracy percentage increased from 76% to 84%. So, there is no improvement in the MA class' recommendation for the application.

Table 4: Confusion matrix and classification accuracy for yield classification using ndvi2\_m and ndvi2\_final attributes

Classification/Original	B-M	M	M-A	Accuracy [%]
B-M	2	0	0	8%
M	20	65	15	85%
M-A	3	10	27	67%

In the above table, you can see that the average municipality yield (as a percentage of raw input) was calculated using only the ndvi2 m and ndvi2 final attributes. Looking at all the master data descriptions (ndvi2 m and ndvi2 final), it was determined that the

highest yields could be achieved with only the ndvi2 m attributes, however, though both the ndvi2 m and ndvi2 final data were not able to demonstrate the plots that were required. It is very critical that the conditions in the field (field adaptation) must be optimal.



**Figure 3:** Decision tree for yield classification using ndvi2\_final and ndvi2\_m attributes

Correlation studies between both the two spectral properties of phase 2 and the mean municipal yield were performed to determine the trend seen in the above graph, in which maximum value are linked to

organizational yield and vice versa. In the first solution to the issue, the alternative under consideration was to determine the average crop yield of a typical municipality for the stated cropping season.

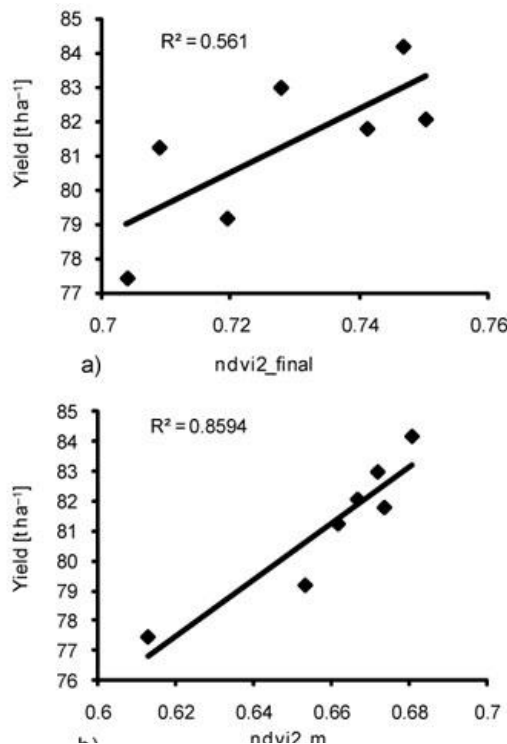


**Figure 4:** a) Correlation between ndvi final in phase 2 and average yield for each cropping season (considering different regions). b) Correlation between average ndvi in phase 2 and average yield for each crop (considering different regions)

The NDVI maps in the accompanying diagram shows that the correlation findings between the final/average NDVI, the NDVI from phase 2, and the total return for each cropping season, considered estimates among different area. Each capped circle in graphs corresponds to one planting season. The findings were consistent with the description provided in the above diagram, i.e., cropping seasons with higher spectral value of a dependent variable appeared to produce higher yields and vice versa.

The goal of this approach was to check whether the regional or seasonal yield historical trend (historical sequence from 2013 to 2020) could be viewed in the electronic spectrometer. The findings shown on the following graph almost match the results of Image 10. The low coefficient of determination may suggest these effects were consistent, considering the low number of patients who were involved in the study. The R2 value for the results in Geouge was predicted to be lower than that of other regions due to the impact of random sampling on the results.

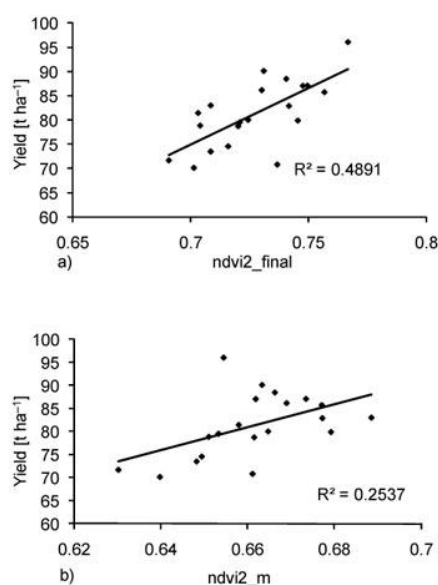


**Figure 5:** a) Correlation between final ndvi in phase 2 and average yield for each region - historical series between 2013 to 2020; b) Correlation between average ndvi in phase 2 and average yield for each region - historical series between 2013 to 2020

## V. CONCLUSION

Despite being higher in accuracy than other standards, they are good indicators for crop monitoring purposes as used by the European Commission (JRC, 2010) as monthly crop bulletin monitoring basis, which produces these bulletins based on NDVI signals, which provide a basis for quantitative assessments of crop growth. The FDA cites a study by CATHERINE AGUSTIN, BA and BRENDA S.H. RANE in which they note that there are various scientific studies on the use of satellite imagery in farming, one of which is the "Development of the Moderate Resolution Imaging Spectroradiometer (MODIS) In Situ (MODIS-I) for Crop Yield Estimation," which examining the ability of satellite imagery to estimate crop yields for rice.

## REFERENCES

- [1] Boken, VK & Shayewich, CF. (2002). Improving an operational wheat yield model using phenological phase-based Normalized Difference Vegetation Index. *International Journal of Remote Sensing*, 23, 4155-4168.
- [2] Left, JCDM, Antunes, JFG; Baldwin, DG; Emery, WJ, & Zullo Júnior, J. (2006). An automatic system for AVHRR land surface product generation. *International Journal of Remote Sensing*, 27, 3925-3942.
- [3] Ferencz, C., Bognár, P., Lichtenberger, J., Hamar, D., Tarcsai, G., Timár, G., Molnár, G., Pásztor, S., Steinbach, P., Székely, B., Ferencz, OE, & Ferencz-Árkos, I. (2004). Crop yield estimation by remote sensing. *International Journal of Remote Sensing*, 25, 4113-4149.
- [4] Greenland, D. (2005). Climate variability and sugarcane yield in Louisiana. *Journal of Applied Meteorology*, 44, 1655-1666.
- [5] Fernandes et al. (2006). *Joint Research Center [JRC]. Meteorological data simulated by ECMWF model*. Available at: <http://mars.jrc.ec.europa.eu/mars/About-us/FOODSEC/Data-Distribution>.
- [6] Joint Research Center [JRC]. (2006). *Bulletins and publications*. Available at: <http://mars.jrc.ec.europa.eu/mars/Bulletins-Publications>.
- [7] Labus, MP, Nielsen, GA, Lawrence, RL, & Engel, R. (2002). Wheat yield estimates using multi-temporal NDVI satellite imagery. *International Journal of Remote Sensing*, 23, 4169-4180.
- [8] Roerink, GJ, Menenti, M., & Verhoef, W. (2000). Reconstructing cloudfree NDVI composites using Fourier analysis of time series. *International Journal of Remote Sensing*, 21, 1911-1917.
- [9] Simões, MS, Rocha, JV, & Lamparelli, RAC. (2005a). Spectral variables growth analysis and yield of sugarcane. *Scientia Agricola*, 62, 199-207.
- [10] Simões, MS, Rocha, JV, & Lamparelli, RAC. (2005b). Growth indices and productivity in sugarcane. *Scientia Agricola*, 62, 23-30.
- [11] Simões, MS, Rocha, JV, & Lamparelli, RAC. (2009). Orbital spectral variables, growth analysis and sugarcane yield. *Scientia Agricola*, 66, 451-461.
- [12] Ali MM, Qaseem MS, Rajamani L, & Govardhan A. (2013). Extracting useful rules through improved decision tree induction using information entropy. *Int. J. Inf. Sci. Techniques*, 3(1), 27-41.
- [13] Alparslan E, Coskun G, & Alganci U. (2009). Water quality determination of Küçükçekmece lake,

Turkey by using multispectral satellite data. *Sci. World J.*, 9, 1215–1229.

[14] Anderson JR, Hardy EE, Roach JT, & Witmer RE. (1976). A land use and land cover classification system for use with remote sensor data. *United States Government Printing Office, Washington, DC.*

[15] Avci ZU, Karaman M, Ozelkan E, & Papila I. (2011). A comparison of pixel based and object-based classification methods, a case study. *Istanbul, Turkey.*

[16] Avery TE & Berlin GL. (1992). *Fundamentals of remote sensing and airphoto interpretation.* Prentice Hall.

[17] Baret F & Guyot G. (1991). Potentials and limits of vegetation indices for LAI and APAR assessment. *Remote Sens. Environ.*, 35, 161-173.

[18] Blackburn GA. (2007). Hyperspectral remote sensing of plant pigments. *J. Exp. Bot.*, 58, 855–867.

[19] Buschmann C & Nagel E. (1993). In vivo spectroscopy and internal optics of leaves as basis for remote sensing of vegetation. *Int. J. Remote Sens.*, 14, 711–722.

[20] Chander G, Markham BL, & Helder DL. (2009). Summary of current radiometric calibration coefficients

for Landsat MSS, TM, ETM+ and EO-1 ALI sensors. *Remote Sens. Environ.*, 113, 893–903.

[21] Congalton RG & Green K. (1999). *Assessing the accuracy of remotely sensed data: principles and practices.* Boca Raton: Lewis Publishers.

[22] Dai QY, Zhang CP, & Wu H. (2016). Research of decision tree classification algorithm in data mining. *Int. J. Database Theory Appl.*, 9(5), 1–8.

[23] Deering DW. (1978). Rangeland reflectance characteristics measured by aircraft and spacecraft sensors. *Ph.D Dissertation. Texas A & M University, College Station*, pp. 338.

[24] Deering DW, Rouse JWJ, Haas RH, & Schell JA. (1975). Measuring forage production of grazing units from Landsat MSS data. In: *10th International symposium on Remote Sensing of Environment*, pp. 1169–1179.

[25] De Fries RS, Hansen M, Townshend JR, & Sohlberg R. (1998). Global land cover classifications at 8 km spatial resolution: the use of training data derived from Landsat imagery in decision tree classifiers. *Int. J. Remote Sens.*, 19(16), 3141–3168.